sLHC-Project-Note-0040

2012-09-18

liu@temf.tu-darmstadt.de

sLHC Project Notes

Cong Liu, Wolfgang F.O. Müller, Wolfgang Ackermann, and Thomas Weiland
Technische Universität Darmstadt, Institut für Theorie Elektromagnetischer Felder (TEMF),
Schlossgartenstrasse 8, 64289 Darmstadt, Germany

Keywords: Field Simulation, Calculation of eigenmodes, RF cavities

Various approaches to electromagnetic field simulations for RF cavities

Summary

In the Superconducting Proton Linac (SPL) cavity, it is very important to calculate the eigenmodes precisely, because many higher order modes (HOMs) can lead to particle beam instabilities. We used and compared three different ways to calculate the eigenmodes in the SPL cavity: field simulation with hexahedron mesh in time domain, field simulation with hexahedron mesh in frequency domain and field simulation with tetrahedral mesh and higher order curvilinear elements. In this paper the principles of the three numerical methods will be introduced and compared. Finally the calculated results will be presented.

1. Introduction

The Superconducting Proton Linac (SPL) [1] at CERN uses two families ($\beta = 0.65$ and $\beta = 1$) of elliptical five cell superconducting cavities. Both families operate at 704.4 MHz. As shown in earlier studies [2], many higher order modes (HOMs) can cause particle beam instabilities. For this reason the properties of higher order modes should be exactly analysed. For this purpose the frequencies of HOMs must be calculated as accurately as possible. In addition, the detailed field distribution of HOMs is also essential to calculate the shunt impedance of the individual mode. In this paper the principles of three numerical methods to field simulation will be introduced and compared. Finally the calculated results will be presented.

2. Field Simulation with Hexahedron Mesh in Time Domain

The first method field simulation with hexahedral grid in time domain should be carried out with Transient Solver from CST MICROWAVE STUDIO® [3]. In order to excite the electromagnetic field in the cavity a broadband high-frequency pulse was coupled into the cavity through a coaxial-type power coupler, furthermore a discrete port was put in the first cell of the SPL cavity. Some probes in x-, y- and z-direction were placed in the fifth cell of the cavity, so that the electromagnetic field in time domain can be detected and recorded (see Fig. 1). After a Fourier transformation of the recorded field data the eigenmode spectrum in frequency domain can be achieved. It is obvious by comparing the results from frequency and time domain, that many eigenmode frequencies are located at the maximums of the

eigenmode spectrum. For example the fundamental passband TM_{010} is shown in Fig. 2. Therefore the frequencies of the eigenmodes can be measured from the eigenmode spectrum. Before the second simulation with the Transient Solver the electric field monitors for the measured frequencies should be defined, so that the field distribution of the eigenmodes (Fig. 3) can be achieved after the second simulation and the corresponding shunt impedance can be determined.

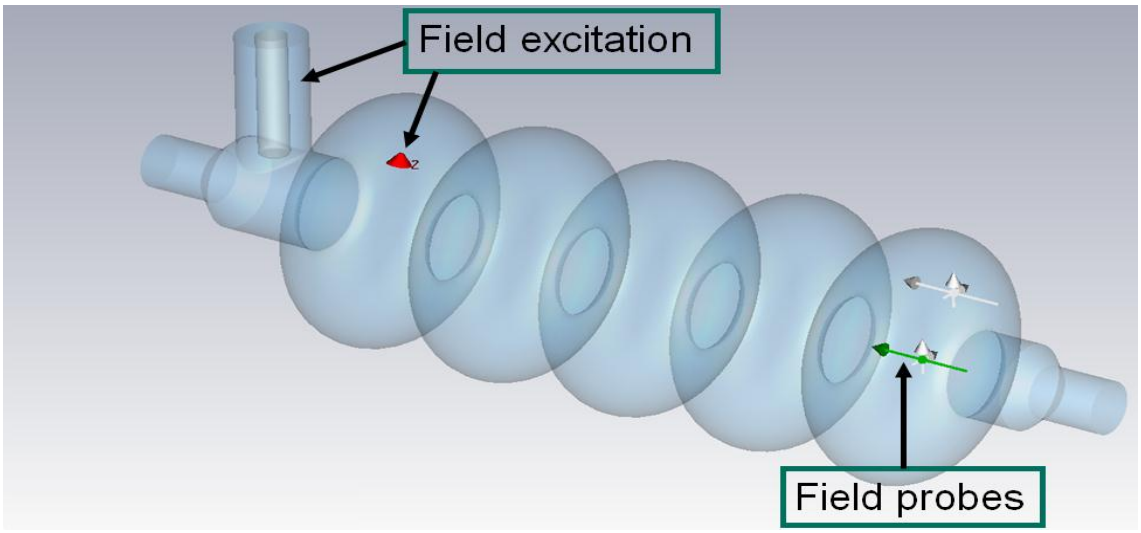

Fig. 1. Power coupler and discrete port in cell 1, Field detection in cell 5.

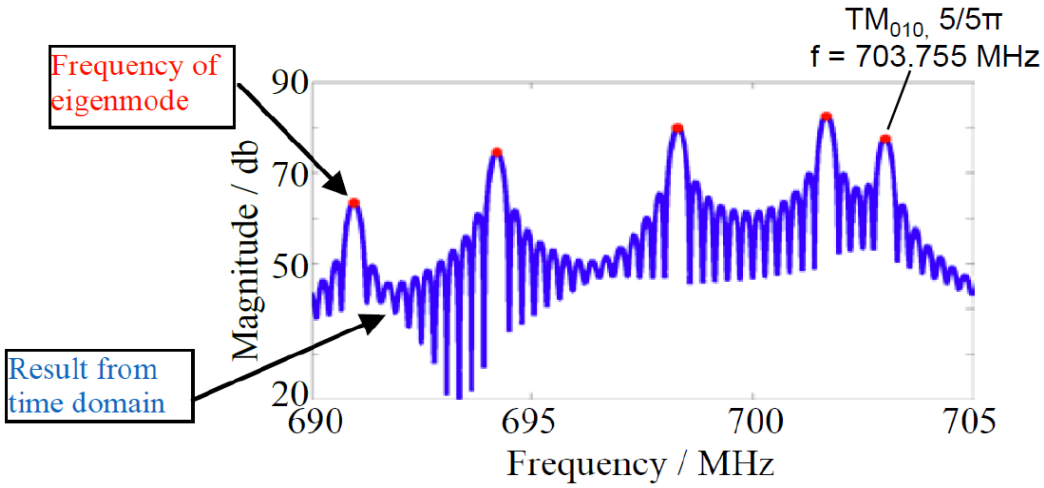

Fig. 2. Eigenmode Spectrum of TM_{010} Passband.

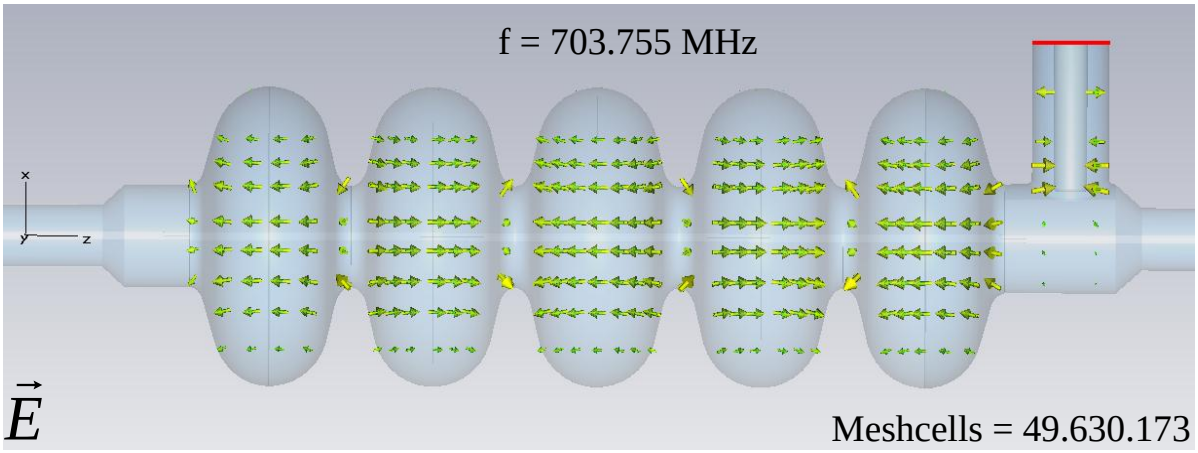

Fig. 3. Field distribution of $TM_{010,}$ π mode (Accelerating mode).

The field simulation from Fig. 2 and Fig. 3 was run with very high resolution (49.630.173 hexahedral elements FPBA), but the calculated frequency for $TM_{010,}$ π mode was 703.755 MHz, smaller than the design frequency (704.4 MHz). Apart from the resonance frequency for the eigenmode, the calculated field components were also not accurate (Fig. 4). The five peaks and minimums of the electric field strength were not located at the same level. Therefore much more hexahedral elements are required to get the accurate eigenmode frequencies and the corresponding electromagnetic field date, which will lead to a time consuming simulation process. For example it took about 50 hours with the GPU cluster to get the results in Fig. 2.

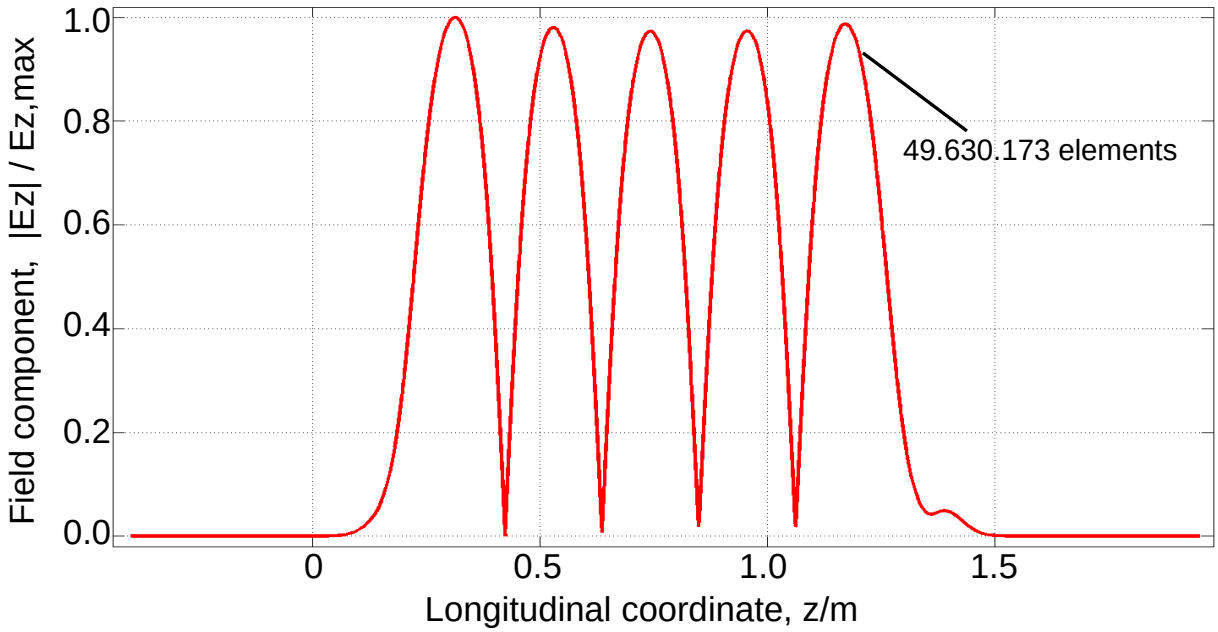

Fig. 4. Evaluation of the electric field strength along the cavity axis. All Cartesian components are normalized to the maximum longitudinal field value Ez,max. The computational mesh consists of 49.630.173 hexahedral elements.

3. Field Simulation with Hexahedron Mesh in Frequency Domain

Compared to the first method the simulation with hexahedral grid in frequency domain is a considerably simpler way to simulate the field in SPL cavity. The eigenmode frequencies and shunt impedances can be calculated with hexahedral discretization directly by the Eigenmode Solver in CST MICROWAVE STUDIO®. The results from the Eigenmode Solver involve the frequencies and the field distribution of the eigenmodes. From that the shunt impedance of the individual eigenmode can be calculated. But similar to the first method a large number of hexahedral grid points for the elliptical SPL cavities are required to achieve stable simulation results, because a lower number of hexahedral elements cannot represent the contours of the elliptical resonator precisely. This can result in a slow convergence of the Eigenmode Solver (Fig. 5 and Fig. 6), which leads to extremely time consuming simulations (Fig. 7). As can be seen from Fig. 5 and Fig. 6, the convergent frequency (80 million hexahedral elements PBA) for $TM_{010,}$ π mode is 704.36 MHz. The convergent value is not very satisfied. In addition the value of the shunt impedance for $TM_{010,}$ π mode was also not convergent. As is indicated in Fig. 7, it took almost 670 hours to run the computation task with 80 million hexahedral elements. Therefore the simulation with hexahedral elements results in a demanding computation task. To solve this problem, accurate curvilinear finite elements, which are able to capture the non-flat shape of typically applied superconducting resonator structures, are used [4].

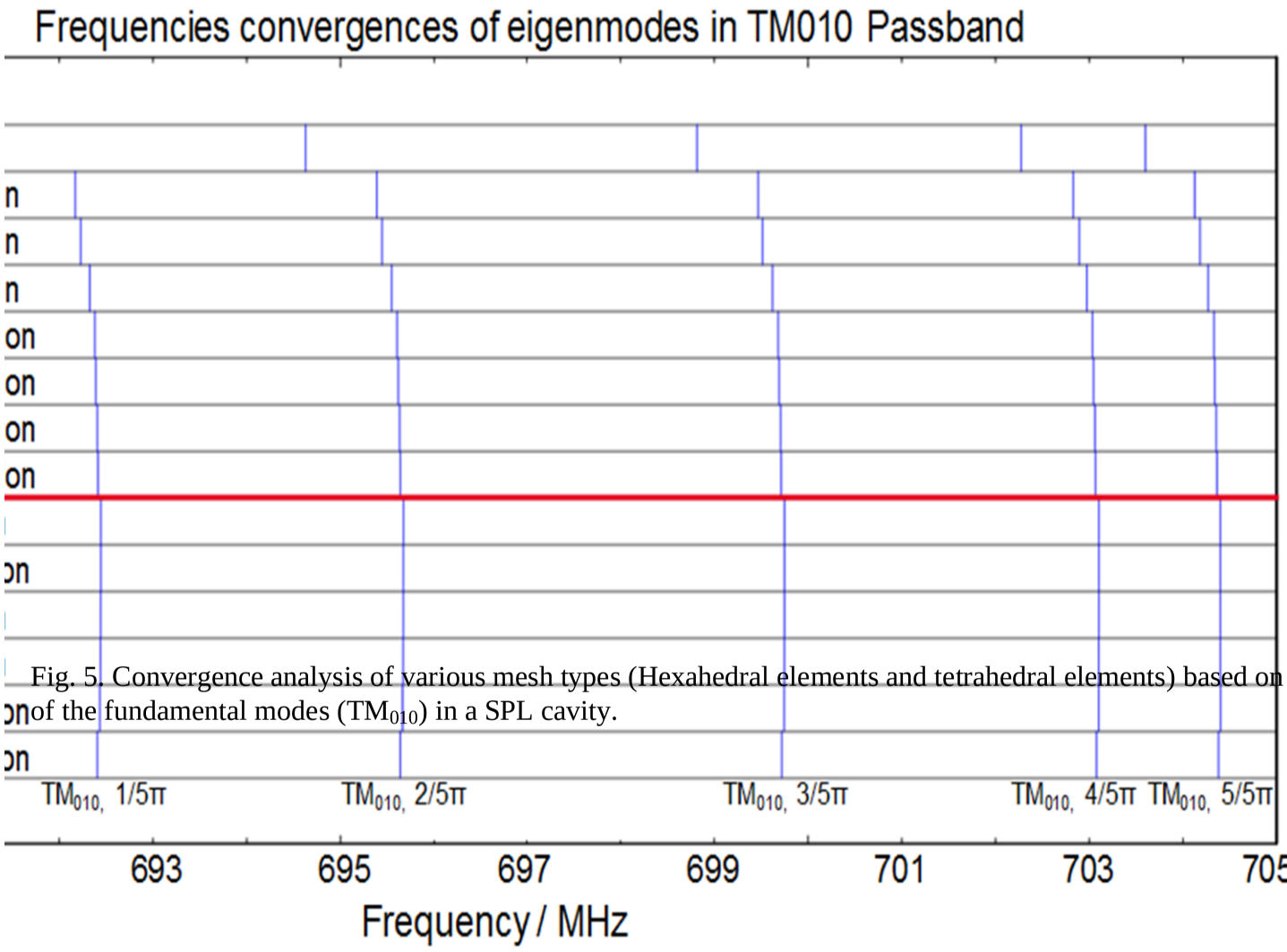

Fig. 5. Convergence analysis of various mesh types (Hexahedral elements and tetrahedral elements) based on the resonance frequency of the fundamental modes (TM_{010}) in a SPL cavity.

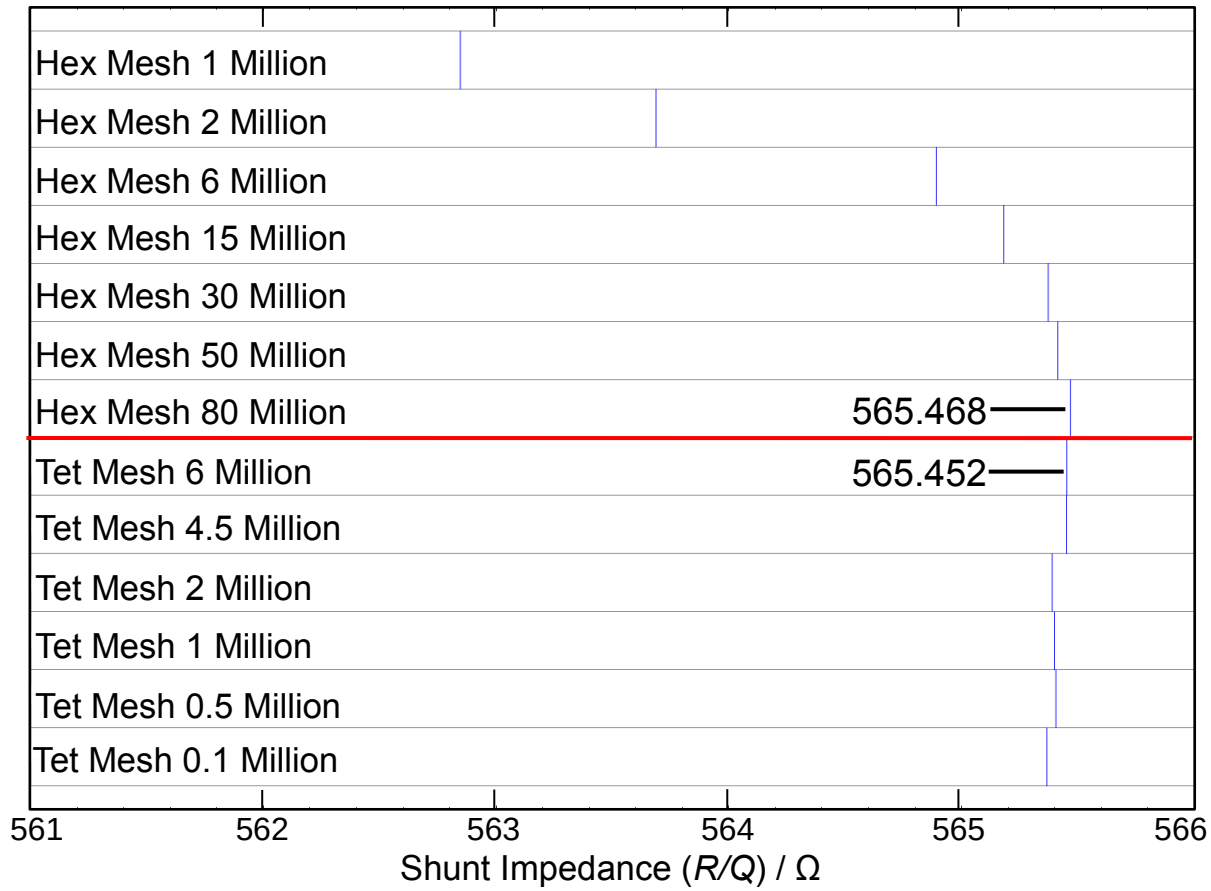

Fig. 6. Convergence analysis of various mesh types (Hexahedral elements and tetrahedral elements) based on the shunt impedance of the fundamental mode ($TM_{010,}$ π) in a SPL cavity.

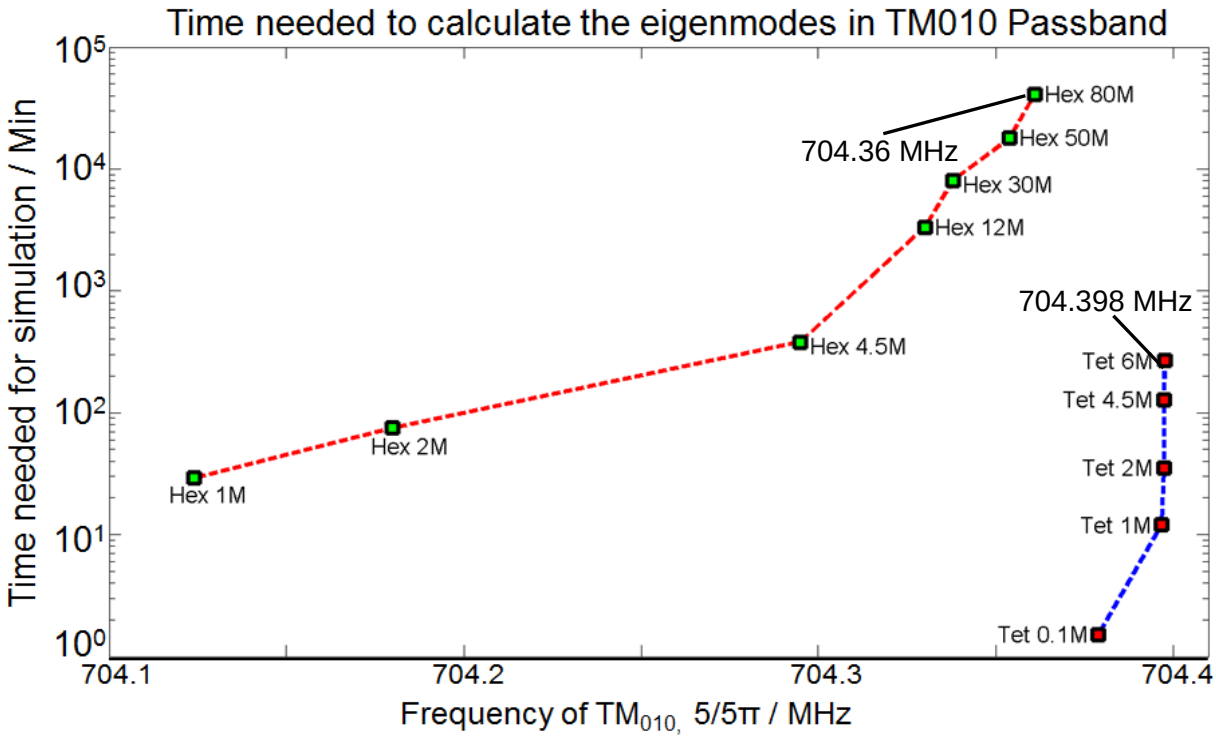

Fig. 7. Simulation time analysis of various mesh types (Hexahedral elements and tetrahedral elements) based on the resonance frequency of the fundamental modes (TM_{010}) in a SPL cavity. (Simulation with hexahedral mesh: single workstation: CPU: 8 processors (Intel Xeon X5472 @3.00GHZ). DRAM: 64GB. Simulation with tetrahedral mesh: MPI cluster: 168 nodes, CPU: 336 processors (Intel Xeon X5650 @2.66GHz), DRAM: 4TB).

4. Field Simulation with Tetrahedral Mesh and Higher Order Curvilinear Elements

A popular discretization method is the Finite Element Method (FEM), which is employing a plain tetrahedral mesh (Fig. 9 (a)) [4]. But in case curved material interfaces (for example, elliptical SPL cavity) have to be considered, the curvilinear elements (Fig. 9 (b)) can be applied to improve high precision modeling [4]. The precise modeling employs huge memory resources and requires long simulation times, therefore it is difficult to run such large computation on classical workstation [4]. To keep the simulation time on an acceptable level, the simulation is run on a distributed memory architecture using the MPI parallelization strategy [4]. The geometric modeling of the SPL cavity structure with the tetrahedral meshing is performed within the CST MICROWAVE STUDIO®. Then the necessary information is passed to the FEM program by means of ASCII or binary file transfer [4]. The entire FEM program is written in C^{++} by Dr.-Ing. Wolfgang Ackermann at the Institut für Theorie Elektromagnetischer Felder (TEMF), Technische Universität Darmstadt.

In Fig. 5 and Fig. 6, the results of the convergence for tetrahedral mesh are displayed. As expected, Fig. 5 shows us a very fast convergence of the eigenmodes frequencies in TM_{010} passband. The convergent value of the frequency for TM_{010}, π mode is also precise (704.397 MHz). According to Fig. 6, compared to the hexahedral elements the value of the shunt impedance for the tetrahedral mesh is convergent. Another advantage for employing the tetrahedral mesh is the acceptable simulation time. As is shown in Fig. 7, using the MPI parallelization strategy the time needed to run the simulation is much more efficient than hexahedral mesh*. Apart from the convergence study of tetrahedral mesh based on the eigenmodes in the fundamental passband, such convergence for higher order modes was analyzed too, for example, the TM_{110} passband (Fig. 8). The convergence of the eigenmodes frequencies was very fast.

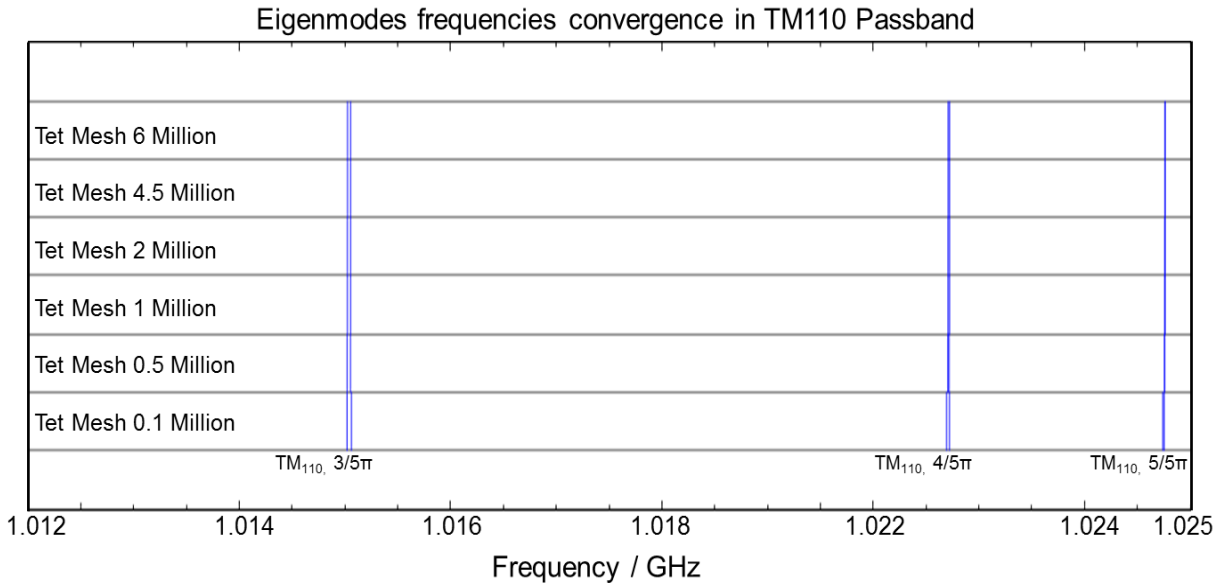

Fig. 8. Convergence analysis of tetrahedral mesh based on the resonance frequency of the TM_{110} modes in a SPL cavity.

---

* Simulation with hexahedral mesh:
single workstation: CPU: 8 processors Intel Xeon X5472 @3.00GHZ. DRAM: 64GB.
Simulation with tetrahedral mesh:
MPI Cluster: 168 nodes: CPU: 336 @processors (Intel Xeon @X5650 2.66GHz), DRAM: 4TB.

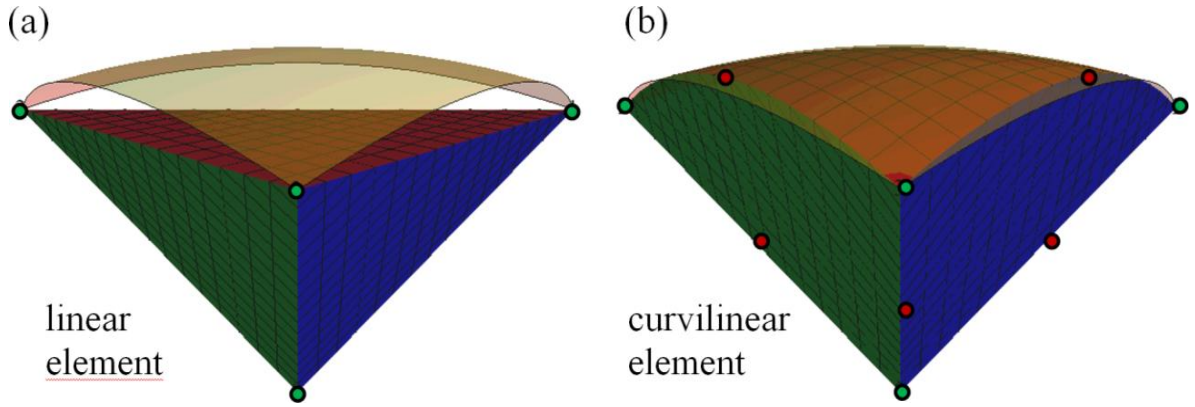

Fig. 9. Linear versus curvilinear tetrahedral element [4].

For the field simulation in the SPL cavity, apart from the eigenmode frequencies also the field distribution demands high precision. In Fig. 10, the calculated field components E_x, E_y and E_z normalized to the maximum longitudinal value $E_{z,max}$ for non-symmetrical tetrahedral mesh and symmetrical tetrahedral mesh are plotted. In a cylindrically symmetric cavity the accelerating mode (TM010, pi) does not have any transverse field components on axis. The only exception in the simulated geometry of the SPL cavities is the area of the power coupler, which is mounted in x-direction, and which therefore introduces a certain transverse field component on axis. Compared to the maximum longitudinal electric field Ez,max the transverse on-axis components in the coupler area are approximately 3 orders of magnitude smaller and they should in fact be zero outside of the region of the coupler. Such large differences in field amplitudes between transverse and longitudinal are difficult to resolve and often lead to numerical noise as depicted in Fig. 10 a) and b). In order to reduce the noise and to improve the accuracy of the shunt impedance calculation, symmetric mesh cells should be involved in the field evaluation process [4]. Tetrahedal grids, which are symmetric to the beam axis (Fig. 11) can be used to suppress the noise as described in the following. According to the results plotted in Fig. 10 c) and d), if the field is evaluated on symmetric mesh, the transverse field components in resonant region are completely eliminated. The transverse components only appeared in the beam pipe, where the power coupler is assembled, because the mesh in this area is non-symmetric. In addition Fig. 10 c) and d) show the quite smooth longitudinal component (E_z), which is applied to accelerate the particle beam. The magnitude difference of E_z between the two mesh types is up to 4 orders.

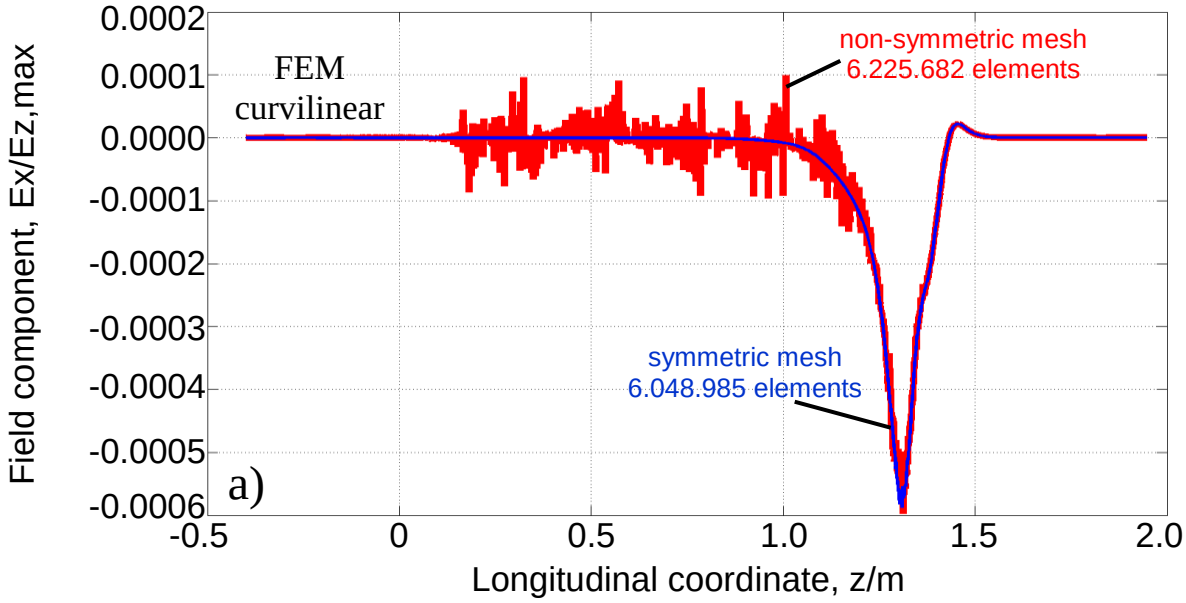

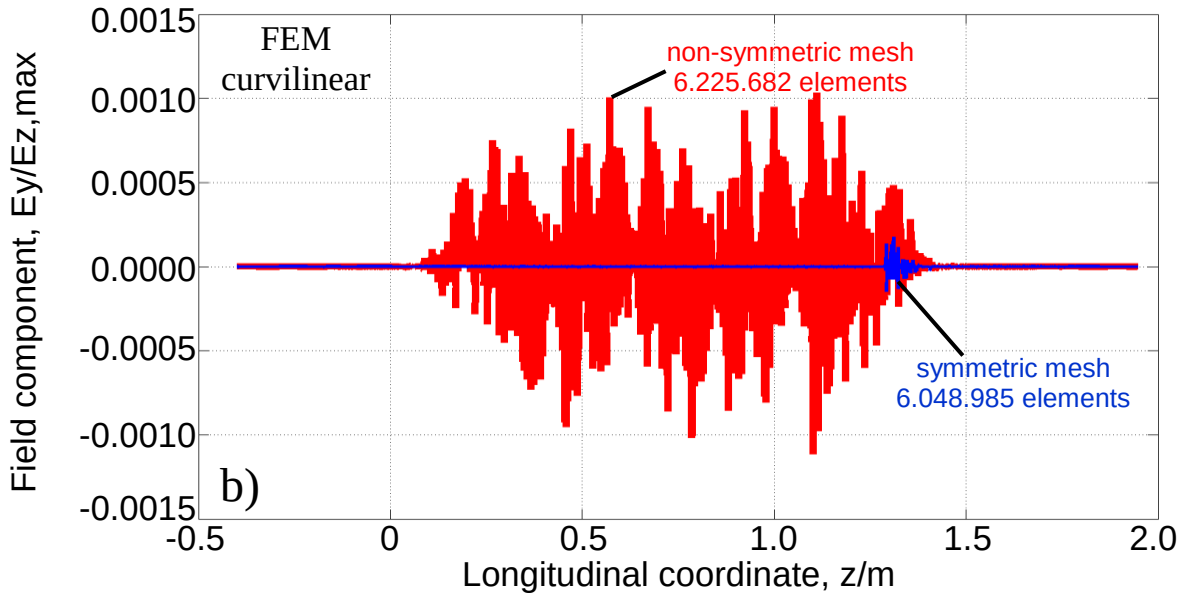

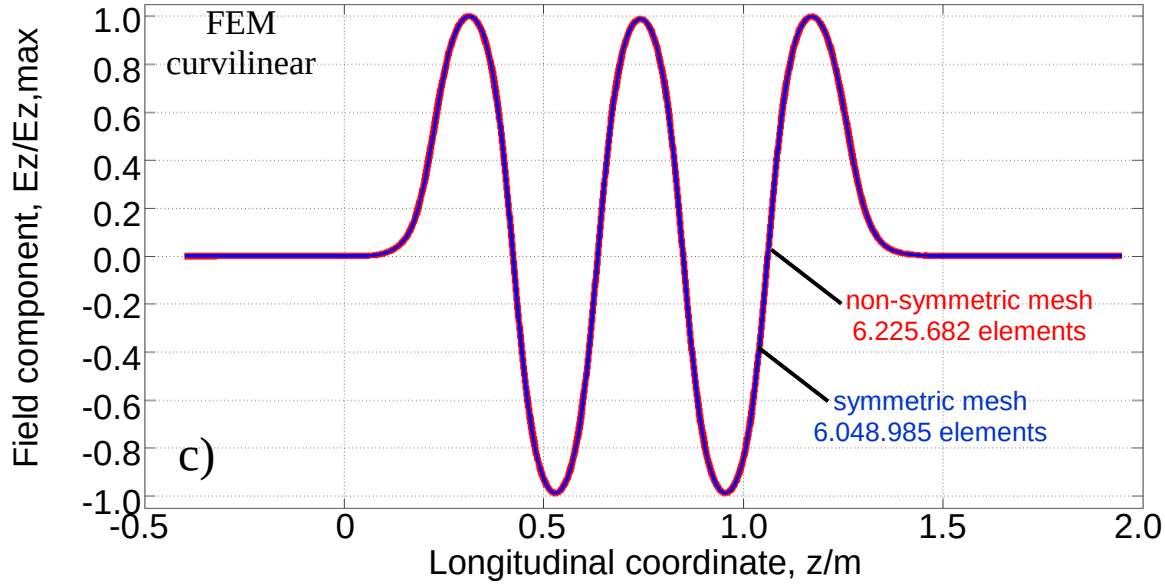

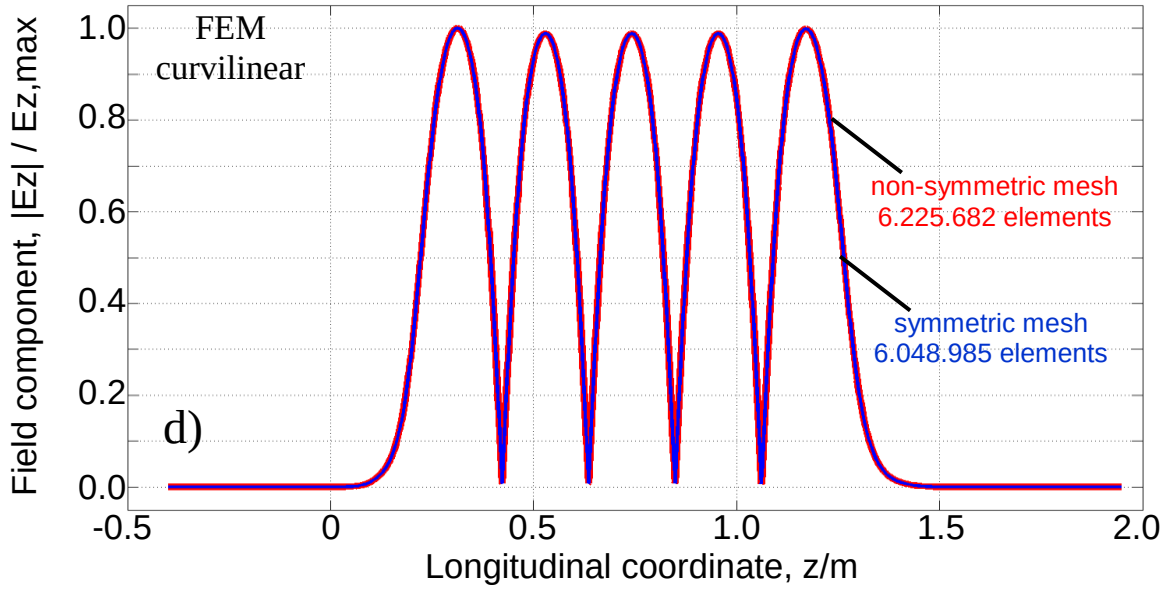

Fig. 10. Evaluation of the electric field strength along the cavity axis. All Cartesian components are normalized to the maximum longitudinal field value Ez,max. All calculations are performed using non-symmetrical and symmetrical curvilinear tetrahedral elements.

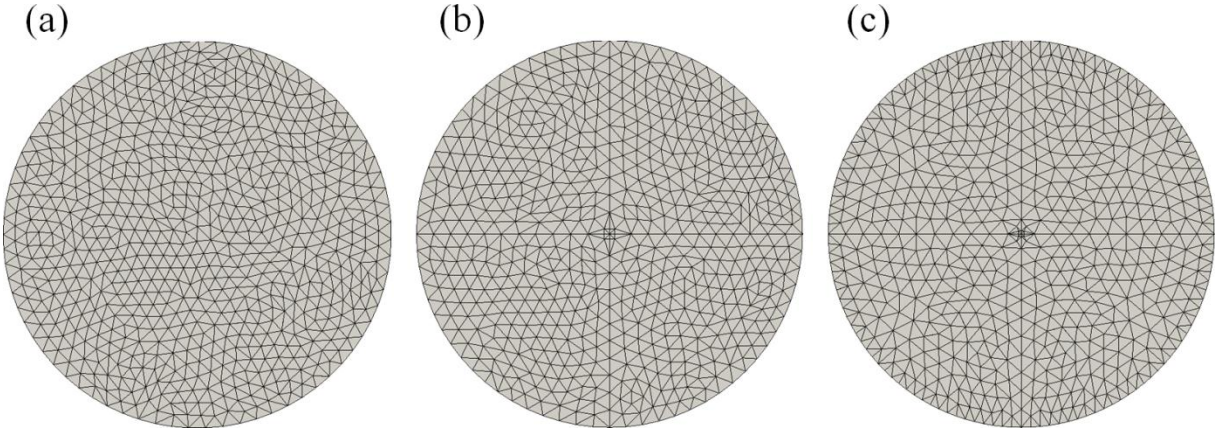

Fig. 11. Cross section of a tetrahedral mesh in a plane normal to the longitudinal axis of the resonator for an arbitrary unstructured mesh (a), a mesh aligned at the coordinate planes (b) and a true symmetric mesh (c) [4].

For the SPL Cavity with couplers a symmetric mesh at least in the resonant region should be generated [4]. Fig. 12 shows us a geometrical model of the SPL cavity, which is used to set up a partially symmetric mesh. At first an initial mesh is generated for ¼ of the model (resonant region). In the next step, the generated tetrahedral elements are mirrored into the missing quadrants [4].

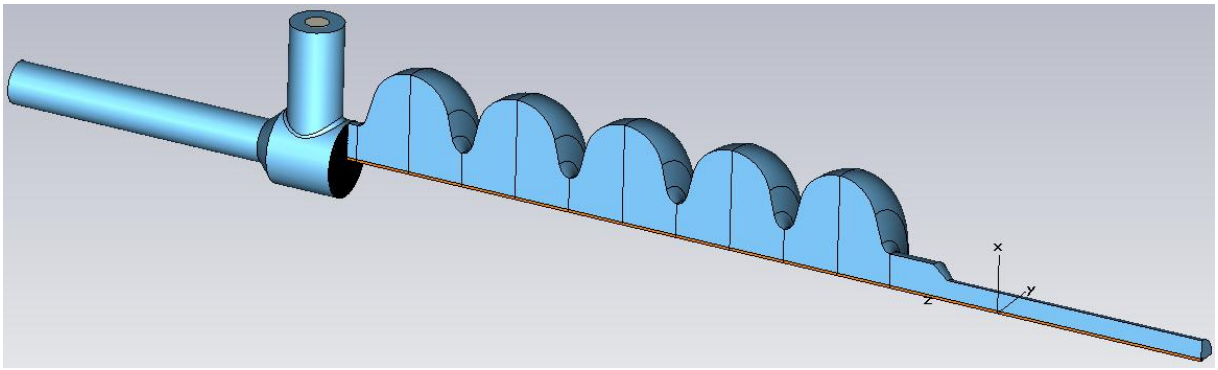

Fig. 12. Geometrical model of the 5-cell SPL cavity used to set up a partially symmetric mesh.

General speaking, the electromagnetic field in an elliptical SPL cavity can be precisely calculated by a parallel FEM eigenvalue solver on the basis of symmetric curvilinear tetrahedral elements. To suppress the transverse components in the beam pipe, where the couplers are assembled, the symmetric tetrahedral mesh will be separately set up in the future.

As is illustrated in above section, apart from the resonance frequency, a further important result of the eigenvalue calculation is the shunt impedance of the eigenmodes. The mode frequencies and the *R/Q* of the TM_{010} modes in the five cell SPL cavities obtained with second order Finite Element approximations are listed in Table I.

TABLE I. TM_{010} passband modes – FEM (Tetrahedral Mesh) results of symmetrical cavities and non-symmetrical cavities with power coupler. The exact geometries are listed in Appendix A and B.

	Symmetrical cavities ($\beta = 1$)		Non-symmetrical cavities ($\beta = 1$)	
Mode	Frequency [MHz]	*R/Q* [Ω]	Frequency [MHz]	*R/Q* [Ω]
$TM_{010,}$ 1/5π	692.435	0.0008	692.446	0.0016
$TM_{010,}$ 2/5π	695.673	0.0110	695.676	0.0366
$TM_{010,}$ 3/5π	699.742	0.0076	699.744	0.0105
$TM_{010,}$ 4/5π	703.092	0.0094	703.101	0.0669
$TM_{010,}$ 5/5π	704.379	561.669	704.398	565.452

It is well known that many higher order modes (HOM) with significant value of *R/Q* can drive beam instabilities; therefore a HOM analysis was done. In Fig. 13 and Fig. 14 the higher order modes with the high *R/Q* values in non-symmetrical cavities are listed respectively.

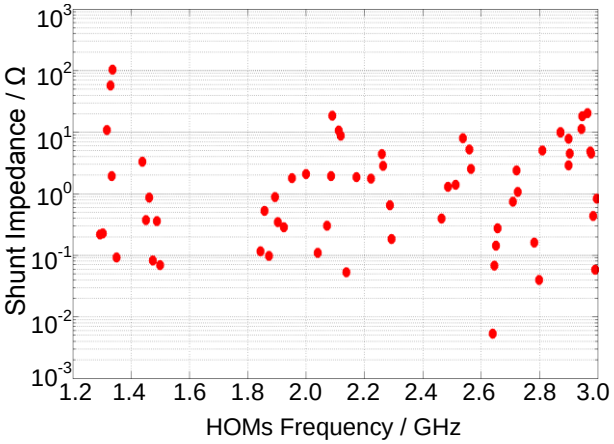

Fig. 13. Longitudinal *R/Q* of monopole eigenmodes in the analyzed non-symmetric cavities.

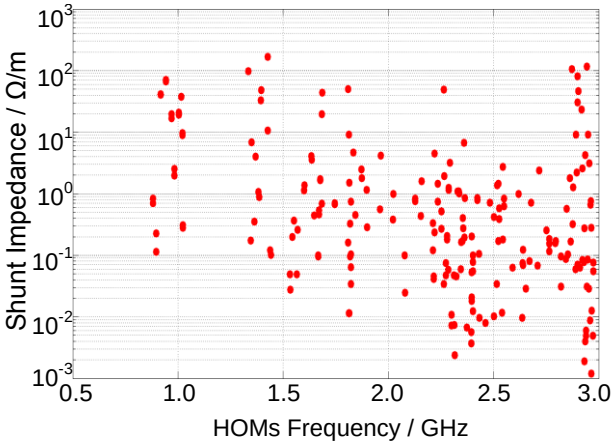

Fig. 14. Transversal *R/Q* of dipole and hybrid eigenmodes in the analyzed non-symmetric cavities.

Apart from non-symmetric cavities with power coupler, the field research for a preliminary symmetrical cavity was also done. The eigenmode analysis was done for a medium beta (β = 0.65) and a high beta (β = 1) cavity. The exact geometries for both types are listed in Appendix B [5]. Table II provides the mode frequencies and the *R/Q* of the five eigenmodes in the fundamental passband. The monopole and dipole modes with the higher *R/Q* values in the considered velocity range for both cavity families are listed in Tables III and IV. These higher order modes have enormous *R/Q* values, which can drive beam instabilities. Such higher order modes must be suppressed through the HOM coupler.

TABLE II. TM_{010} passband modes – FEM (Tetrahedral Mesh) results of symmetrical cavity for medium beta (β = 0.65) and high beta (β = 1) cavity.

	Symmetrical cavity (β = 0.65)		Symmetrical cavity (β = 1)	
Mode	Frequency [MHz]	*R/Q* [Ω]	Frequency [MHz]	*R/Q* [Ω]
$TM_{010,}$ 1/5π	697.409	0.0046	692.435	0.0008
$TM_{010,}$ 2/5π	699.335	0.0068	695.673	0.0110
$TM_{010,}$ 3/5π	701.715	0.0518	699.742	0.0076
$TM_{010,}$ 4/5π	703.642	0.8930	703.092	0.0094
$TM_{010,}$ 5/5π	704.392	318.642	704.379	561.669

TABLE III. Monopole modes with the higher *R/Q* values in symmetrical SPL cavity. The TM_{010} modes are listed in Table II.

Symmetrical cavity (β = 0.65)			Symmetrical cavity (β = 1)		
Mode	Frequency [MHz]	$(R/Q)_{max}$ [a] [Ω]	Mode	Frequency [MHz]	$(R/Q)_{max}$ [a] [Ω]
$TM_{020,}$ 1/5π	1502.69	5.642	$TM_{011,}$ 4/5π	1327.66	35.22
$TM_{020,}$ 2/5π	1509.04	13.92	$TM_{011,}$ 5/5π	1332.32	140.6
$TM_{011,}$ 3/5π	1771.69	7.068	TM_{021}	2088.33	7.69
$TM_{011,}$ 4/5π	1778.70	14.06	TM_{021}	2089.67	23.04
$TM_{011,}$ 5/5π	1781.65	50.12			

[a]Maximum value in covered velocity range.

TABLE IV. Dipole modes with the higher transversal *R/Q* values in symmetrical SPL cavity.

Symmetrical cavity ($\beta = 0.65$)			Symmetrical cavity ($\beta = 1$)		
Mode	Frequency [MHz]	$(R/Q)_{max}$ [a] [Ω/m]	Mode	Frequency [MHz]	$(R/Q)_{max}$ [a] [Ω/m]
TM_{110}	1014.25	112.4	TE_{111}	894.81	20.21
TM_{110}	1018.82	54.53	TE_{111}	915.09	45.52
TM_{110}	1025.36	22.49	TE_{111}	939.35	62.57
TM_{110}	1031.92	8.972	TE_{111}	965.62	22.30
TE_{111}	1267.65	10.78	TM_{110}	1003.44	16.45
			TM_{110}	1014.58	35.77
			TM_{110}	1020.34	19.07

[a]Maximum value in covered velocity range.

At last Fig. 15 and Fig.16 describe the change of *R/Q* as a function of the beam velocity for the symmetrical cavity. The both charts reveal that only a few modes have a nearly constantly high *R/Q* value in the high beta cavity. The *R/Q* value of the eigenmodes can differ several orders of magnitude from the maximum (*R/Q*) in the covered velocity range. In the medium beta cavity few modes have a constantly high *R/Q* value.

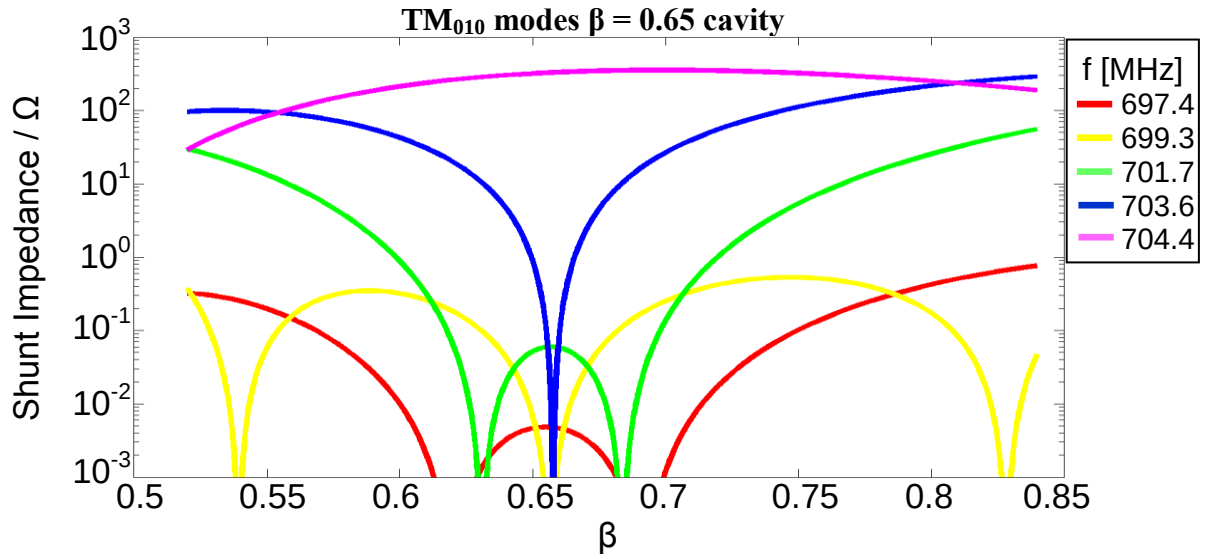

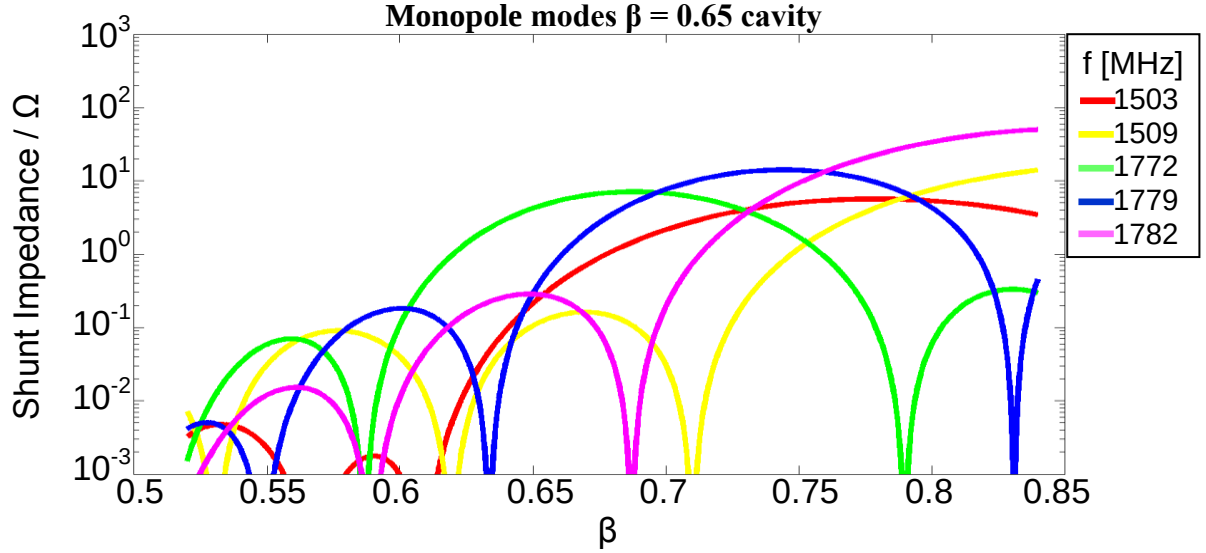

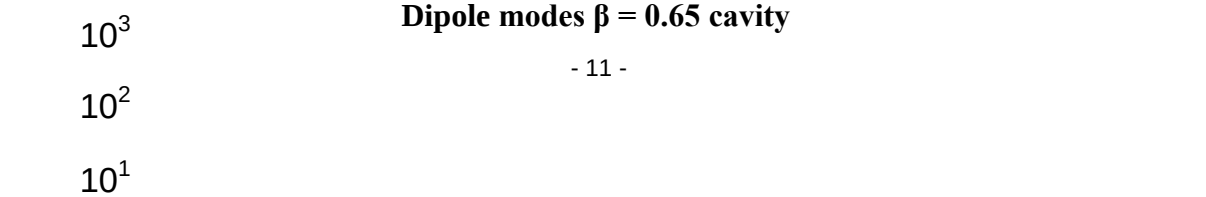

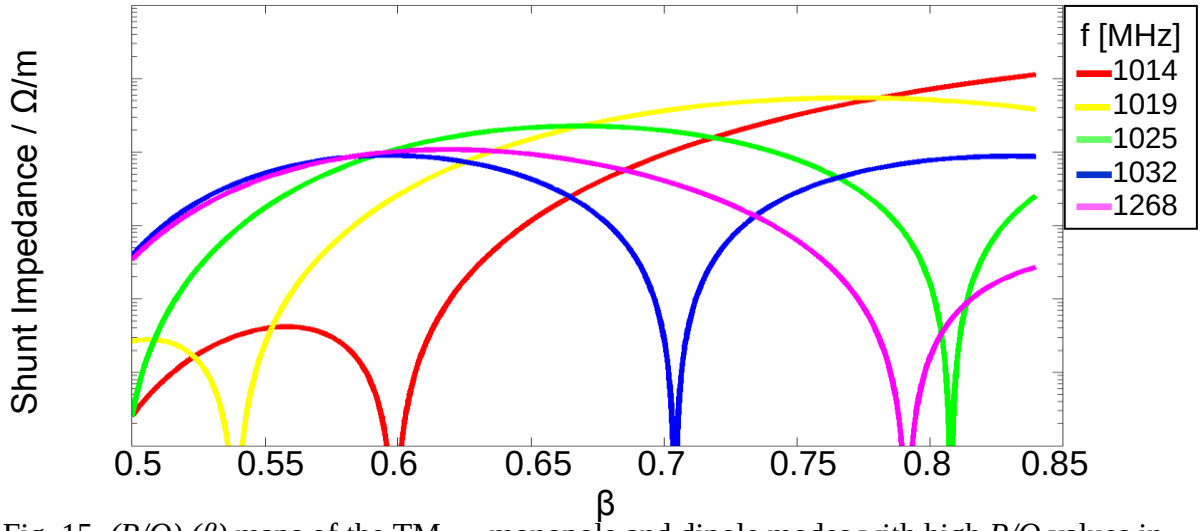

Fig. 15. *(R/Q) (β)* maps of the TM_{010}, monopole and dipole modes with high *R/Q* values in the symmetric medium beta (β = 0.65) SPL cavity.

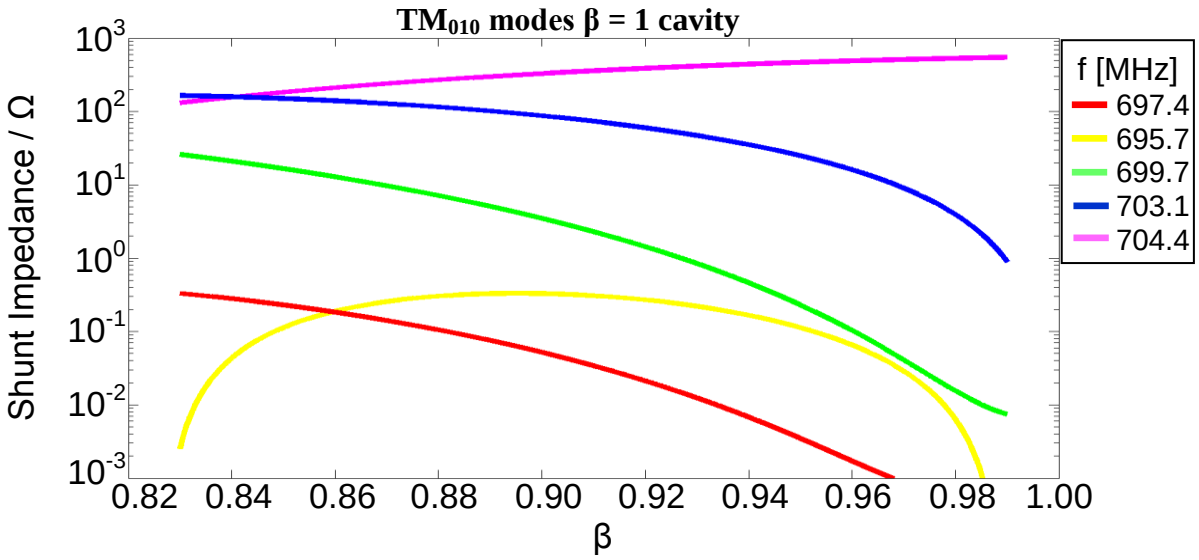

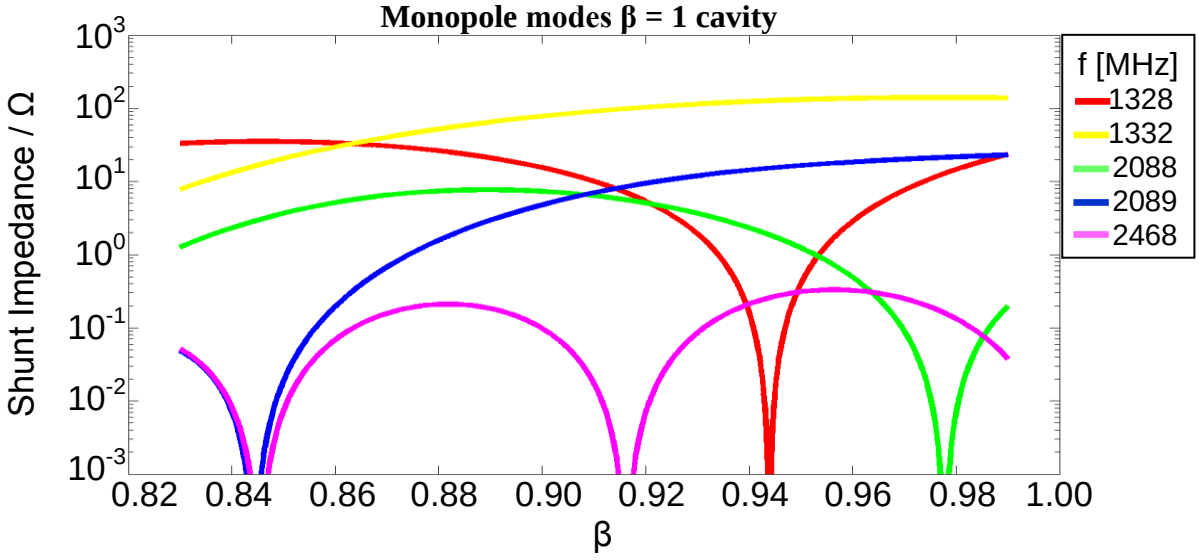

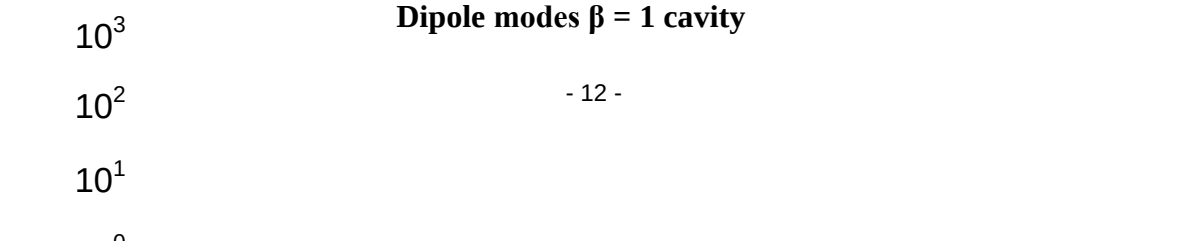

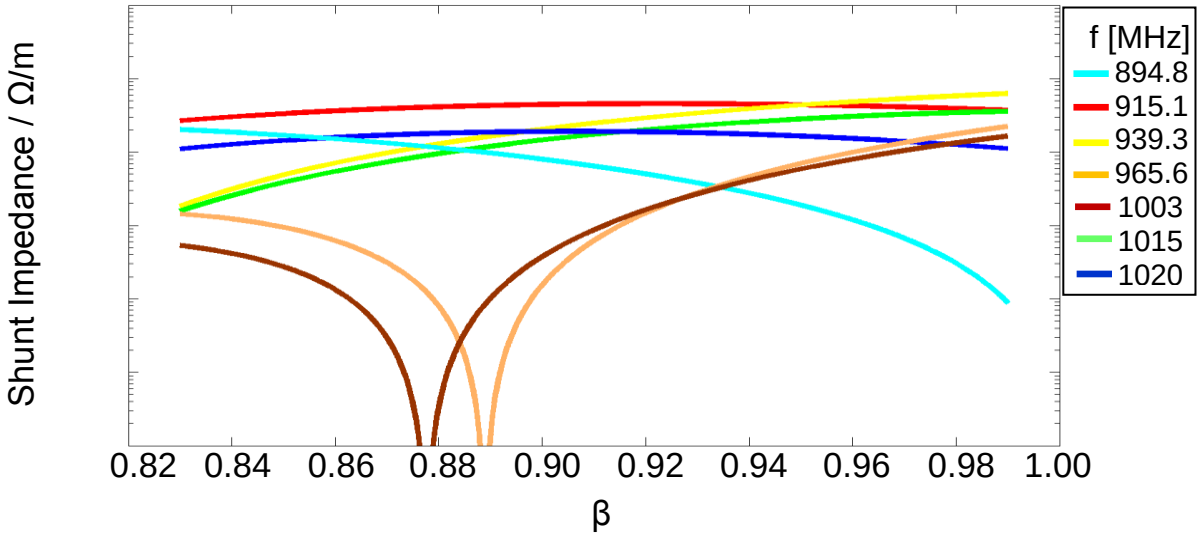

Fig. 16. *(R/Q) (β)* maps of the TM_{010}, monopole and dipole modes with high *R/Q* values in the symmetric high beta ($\beta = 1$) SPL cavity.

5. Conclusion

In this paper three numerical methods to calculate the electromagnetic field in the elliptical SPL Cavity are reported. The numerical methods on the basis of hexahedral elements are not ideal approaches to electromagnetic field simulation for elliptical SPL cavity, because with hexahedral elements it is difficult to match the contours of the elliptical resonator precisely. Furthermore a huge number of the hexahedral elements will lead to a time consuming simulation process and very poor convergence of the simulation results. By comparison a parallel FEM method on the basis of curvilinear tetrahedral elements is able to evaluate the electromagnetic field in the elliptical SPL Cavity precisely and efficiently. The superior convergence rate can be preserved. In addition parasitic high frequency oscillations in the transverse field components along the particle beam axis can be eliminated by using a symmetric arrangement of the tetrahedral elements with respect to the particle beam axis in the cavity region [4]. In the future the symmetric tetrahedral mesh will be separately set up in the beam pipe, where the couplers are assembled, so that the transverse components in the beam pipe can be completely suppressed.

Appendix A: Non-symmetric Cavity Shape Parameters

The non-symmetric cavity shape parameters (including power coupler) are illustrated in Fig. 17, 18, 19 and Table V.

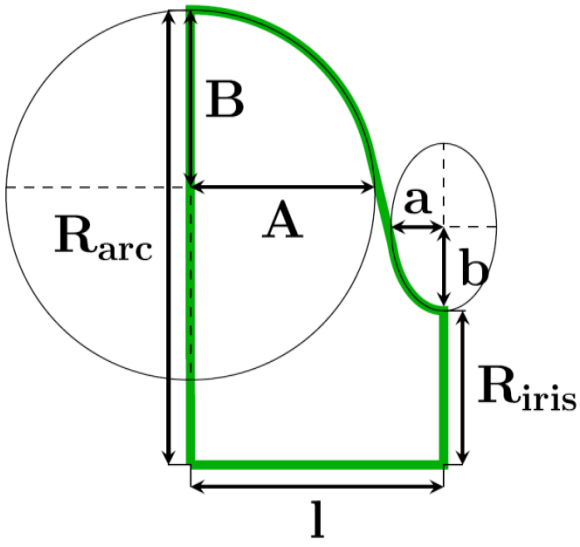

Fig. 17. Cavity with labels of the shape parameters used in Table V and VI [5].

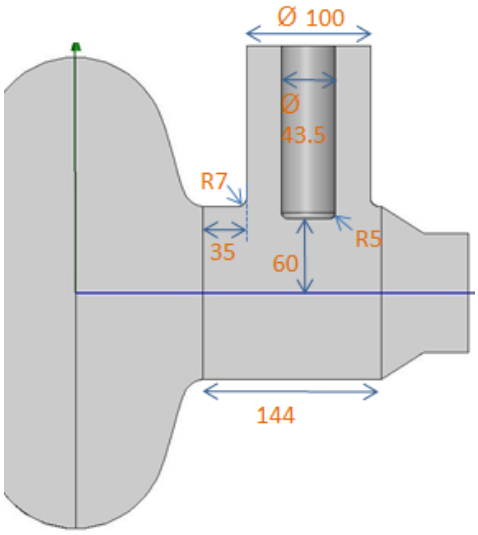

Fig. 18. Shape and position parameters of the power coupler (antenna) [6].

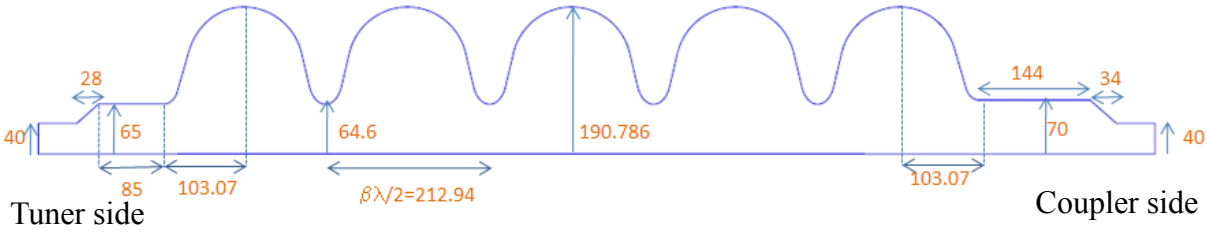

Fig. 19. Shape and position parameters of the beam pipes on the tuner and coupler side [6].

TABLE V. Shape parameters of the non-symmetric five cell elliptical SC cavities. All values are given in mm [6].

Cavity	$\beta = 1$		
Cell	end ½ cell tuner side	mid ½ cell	end ½ cell coupler side
R_{arc}	190.786	190.786	190.786
R_{iris}	65	64.6	70
l_{cell}	103.07	106.47	103.07
A	74.45	77.5	74.45
B	83.27	77.5	76.89
a	18.5	22.1	18.5
b	24.9	35.1	24.9

Appendix B: Symmetric Cavity Shape Parameters

The symmetric cavity shape parameters are illustrated in Fig. 17 and Table VI.

TABLE VI. Shape parameters of the medium and high beta symmetric five cell elliptical SC cavities. All values are given in mm [5].

Cavity	$\beta = 0.65$		$\beta = 1$	
Cell	mid	end	mid	end
R_{arc}	186.4	186.4	190.8	190.8
R_{iris}	45.0	45.0	64.6	70
l_{cell}	70.0	70.0	106.5	103.0
A	45.1	45.1	77.5	76.9
B	45.1	49.6	77.5	74.5
a	12.1	12.1	22.1	18.5
b	15.8	15.7	35.1	24.9

REFERENCES

[1] O. Brunner et al., ”Assessment of the basic parameters of the CERN Superconducting Proton Linac”, Phys. Rev. ST Accel. Beams 12, 070402 (2009).

[2] H. Padamsee, J. Knobloch and T. Hays, “RF Superconductivity for Accelerators”, Second Edition, Wiley-VCH, Weinheim, 2008.

[3] CST MICROWAVE STUDIO®, CST AG, Darmstadt, Germany, www.cst.com.

[4] W. Ackermann, G. Benderskaya and T. Weiland, “State of the Art in the Simulation of Electromagnetic Fields based on Large Scale Finite Element Eigenanalysis”, Technical Article.

[5] M. Schuh, F. Gerigk, J. Tueckmantel, and C P. Welsch, “Influence of higher order modes on the beam stability in the high power superconducting proton linac”, Phys. Rev. ST Accel. Beams 14, 051001 (2011).

[6] J. Plouin, S. Chel, G. Devanz, “SPL cavity design by CEA-Saclay”, 3rd SPL Collaboration Meeting, CERN, France.